First-principles calculations of the structural, phonon and thermal properties of ZnX (X = S, Se,Te) chalcogenides

Article *in* Physica Scripta · May 2014

DOI: 10.1088/0031-8949/89/7/075704

CITATIONS
12

READS
345

4 authors, including:

A. S. Verma
Banasthali University
106 PUBLICATIONS **744** CITATIONS

SEE PROFILE

Dr. S. Sharma
32 PUBLICATIONS **175** CITATIONS

SEE PROFILE

APP Template V1.30 Article id: ps479978 Typesetter: MPS Date received by MPS: 30/04/2014 PE: MAC003313 CE :

IOP Publishing | Royal Swedish Academy of Sciences Physica Scripta

Phys. Scr. **00** (2014) 000000 (9pp)

First-principles calculations of the structural, phonon and thermal properties of ZnX (X = S, Q1 Se,Te) chalcogenides

B K Sarkar[1], A S Verma[2], S Sharma[2] and S K Kundu[1]

[1] Department of Physics, Galgotias University, Gautam Budh Nagar-201308, India
[2] Department of Physics, Banasthali Vidhyapith, Rajasthan 304022, India

E-mail: bks@physics.org.in

Received 7 October 2013, revised 21 February 2014
Accepted for publication 25 April 2014
Published DD MM 2014

Abstract

Zinc chalcogenides, ZnX (X = S, Se and Te), are investigated with the full-potential linear-augmented plane wave (FP-LAPW) method within the framework of the density functional theory (DFT) for their structural, phonon and thermal properties. We consider the generalized gradient approximation (GGA) for the purpose of exchange-correlation energy (Exc) determination. Murnaghan's equation of state (EOS) is used for volume optimization by minimizing the total energy with respect to the unit cell volume. The elastic constants are calculated to examine the crystal structure stability, binding properties and bond character of zinc chalcogenides. By means of frozen-phonon method within the harmonic approximation, we work out phonon dispersion, lattice dynamics and thermal properties of ZnX compounds. The phonon frequencies in the first Brillouin zone (BZ), at the zone centre (Γ) and at the zone boundary (X or L) are estimated. The calculated lattice parameters and thermal parameters are in good agreement with other theoretical calculations as well as with the available experimental data.

Keywords: density functional theory, FP-LAPW+l0, Zn-chalcogenides, phonon dispersion, thermal properties

SQ1 (Some figures may appear in colour only in the online journal)

1. Introduction

During the last decade, a great deal of attention has been devoted to the study of ZnX chalcogenides (X = S, Se, Te) as a member of the broad band gap semiconductor family. They have been shown much interest from a technological point of view and they have gained a reputation for their applications in a variety of opto-electronic devices such as light-emitting diodes, photovoltaic detectors, optical wave guides, modulators and lasers. In particular, zinc selenium, having the distinct property of reversible transformation [1], is utilized in the manufacturing of optical memory devices. These chalcogenides are broadly used for diverse applications in numerous fields such as optical recording due to their excellent sensitivity in laser writing and photography. They have a variety of electrographic applications, such as photoreceptors in photocopying, laser printing, infrared spectroscopy and fibre-optic techniques [2, 3]. From the perspective of semiconductor device technology, it is essential to get detailed knowledge of the different properties of these materials, especially in the design of ZnX-based optoelectronic devices. In recent times, these compounds have been widely studied experimentally for their structural and optical properties [4–8].

Based on density functional theory (DFT) [9], the electronic, structural, dynamical and optical properties for Zn chalcogenides have been extensively studied [10–15]. DFT with a local density approximation (LDA) [16] of the exchange correlation energy has been used for optical properties calculations. The linear muffin-tin orbital model [11] has determined the electronic structures of ZnX compounds. The empirical pseudopotential method has been exploited for

Table 1. The calculated lattice constant (a_0), bulk modulus (B_0) and its pressure derivative B_0' for ZnX compounds compared to other works.

Compound	a_0 (A°)	B_0 (GPa)	B_0'
ZnS			
Present	5.371	90.12	4.32
Calc.	5.460[a], 5.581[b], 5.302[c], 5.313[d], 5.342[e], 5.3998[f], 5.458[g]	87.835[a], 91.71[b], 77.3[h]	4.455[a], 5.0[i]
Expt.	5.412[l]	75[l]	4.00[l]
ZnSe			
Present	5.632	72.42	4.76
Calc.	5.746[a], 5.690[b], 5.608[i], 5.743[j], 5.568[k], 5.571[k], 5.587[k], 5.624[e]	72.494[a], 73.91[b], 74[i]	4.844[a], 5.0[i]
Expt.	5.667[m]	69.3[m]	
ZnTe			
Present	6.198	60.39	4.71
Calc.	6.194[a], 6.218[b], 6.030[i], 6.187[j], 6.00[e], 6.063[f], 6.195[g]	55.446[a], 55.56[b], 55.900[i]	4.988[a], 5.1[b]
Expt.	6.103[n]	50.9[n]	5.04[n]

[a] [Ref. 31].
[b] [Ref. 32].
[c] [Ref. 33].
[d] [Ref. 34].
[e] [Ref. 13].
[f] [Ref. 11].
[g] [Ref. 14].
[h] [Ref. 35].
[i] [Ref. 36].
[j] [Ref. 44].
[k] [Ref. 37].
[l] [Ref. 45].
[m] [Ref. 39].
[n] [Ref. 46].

the determination of band structure and of the density of states for the ZnX binary compound [13]. The optical spectra have been investigated [17] by solving the Bethe–Salpeter equation. The full potential linearized augmented plane-wave method plus local orbitals (FP-LAPW+l_0) has been used for band-structure calculations [18, 19]. FP-LAPW+l_0 is a very efficient method to identify not only the energy location of the Zn 3*d* electrons and associated band parameters, but also to address the optical response. The *ab initio* full potential with linear muffin-tin orbital methods within LDA [20, 21] and the projector-augmented wave (PAW) method [18, 19] have been used for the calculation of the electronic properties of the ZnO wurzite structure. But the order of states at the top of the valence band (VB), the location of the Zn 3d band and its width do not agree well with experimental values. All these analyses have been done so far mainly for the study of electronic and optical properties. Comparatively Less research has been devoted to the study of the thermal properties of chalcogenides, and few reports describe the lattice dynamics. An *ab initio* calculation was performed for the investigation of the lattice dynamics for Zn-based semiconductors [10]. First-principles calculations of the electronic structure of ZnO determined its structural and lattice-dynamical properties [12]. You Yu *et al* reported the dielectric and dynamical properties of zinc-blende ZnX compounds [22] based on density-functional theory using the pseudopotential method. The pseudopotential method is challenging for systems with localized d- or f-electrons in DFT calculations, as nuclear potential and core electrons are replaced by a useful potential as felt by the valence electrons. On the other hand, the all-electron method [23] describes core and valence electrons on an equal footing. In this method, the space is partitioned into two parts: one is non-overlapping spheres centered at the atomic sites, known as muffin-tin (MT) spheres, and the other is the interstitial region (IR). The spheres confine the core states, treated as localized states in a spherically symmetric atomic potential. In the IR, valence electrons are described by basis functions, which are defined by piecewise plane waves of all reciprocal lattice vectors up to the maximal momentum G_{max}, The plane waves are augmented by radial functions in the MT spheres. Based on the scalar relativistic approximation, the spherically averaged effective potential is estimated. This procedure has been demonstrated to be very accurate for ground-state calculations. Lattice dynamic properties are calculated in two ways: the linear response approach based on the density functional perturbation theory [24], and direct-force constant method or super cell method [25]. Based on density-functional perturbation theory, the phonon band structure is obtained by computing the Fourier transform of dynamical matrices on a regular mesh of wave vectors. In the direct method, the atoms within a super cell are displaced to construct the dynamical matrix. The force constants are calculated via a self-consistent supercell approach in the local-density approximation and the phonon properties are determined.

The objective of this paper is to employ the full-potential linear-augmented plane wave (FP-LAPW) method in the framework of density functional theory (DFT) for the investigation of the structural, electronic, phonon dispersion and thermal properties of ZnX compounds. The exchange-correlation energy (Exc) is determined in the Kohn–Sham calculation by the standard generalized gradient approximation (GGA) parameterized by the Perdew, Burke and Ernzerhof (PBE) or GGA/PBE method. Murnaghan's equation of state (EOS) is considered for volume optimization by minimizing the total energy with respect to the unit cell volume. Based on the direct force constant method [25] with supercell calculations, lattice dynamics and phonon dispersions are analysed. The thermodynamic parameters, including the phonon contribution to the Helmholtz free energy ΔF, the entropy S and the constant volume specific heat C_V, are estimated from the calculated phonon dispersion relations.

2. Computational details

The structural and electronic properties of the compound ZnX are studied by the full potential linearized augmented plane

wave plus local orbitals (FP-LAPW+*lo*) method with Wien2k code [26]. The generalized gradient approximation (GGA) parameterized by Perdew, Burke and Ernzerhof (PBE) [27] is used. By the optimization of the total energy with respect to the unit cell volume using Murnaghan's equation of state [28], the equilibrium structural parameters are estimated. The calculations are performed with $R_{MT}k_{max} = 7$, to accomplish energy eigenvalue convergence, where R_{MT} is the smallest radius of the muffin-tin (MT) spheres and k_{max} is the maximum value of the wave vector. The maximum value of the angular momentum l_{max} is taken as 10 for the wave function expansion inside the atomic spheres. The k-points used in the computational work are taken as a $10 \times 10 \times 10$ Monkhorst–Pack model [29] in the irreducible Brillouin zone (BZ) of the zinc-blende structure. The iteration procedure is continued with the total energy and charge convergence to 0.0001Ry and 0.001e, respectively.

Phonon calculations are carried out within the framework of the direct method. In a $2 \times 2 \times 2$ supercell, real space force constants are calculated from forces on atoms due to changes between equilibrium and distorted structures by using the Wien2k code. The phonon modes are estimated from the force constants using the Phonopy package [30]. The phonon frequencies are determined from forces as a consequence of the displacements of atoms in the supercell.

3. Results and discussion

3.1. Structural properties

Using Murnaghan's equation of state [28], the total energy versus the unit cell volume variation yields to fitting parameters, viz., the equilibrium lattice parameter (a_0), the bulk modulus B_0 and the pressure derivative of the bulk modulus, B_0', for the zinc-blende structure ZnX compounds. The same parameters are displayed in table 1. The energy minima occurs at the values of $a_0 = 5.371$, 5.632 and 6.198 Å for ZnS, ZnSe and ZnTe, respectively. Our results are very close to other calculated values [31–37]. Also the calculated lattice constants agree well with the experimental values of 5.412, 5.667 and 6.103 Å, respectively, with the maximal error of 1.53%. It is obvious that well-defined structural properties are helpful for the further study of electronic and dynamic properties.

To understand of the structural stability, it is necessary to know the values of elastic constants. We have determined the elastic constants of ZnX compounds with a cubic structure using the method developed by Charpin incorporated in the Wien2k code [38]. By applying appropriate lattice distortions in a cubic lattice, three independent elastic constants, C_{11}, C_{12}, and C_{44}, are determined. For the calculation of the elastic constants, the following three equations are considered:

$$B_0 = \left(C_{11} + 2C_{12}\right)/3 \tag{1}$$

$$\Delta E_{rhomb} = \frac{1}{6}\left(C_{11} + 2C_{12} + 4C_{44}\right) V_0 \delta^2 \tag{2}$$

Table 2. The calculated values of the elastic constants (C_{ij} in GPa) at equilibrium for the ZnX compound.

	C_{11}	C_{12}	C_{44}
ZnS			
Present	111	71	69
Expt.[b]	104	65	46.2
ZnSe			
Present	91	63	59
Expt.[a]	85.9	50.6	40.6
ZnTe			
Present	79	48	41
Expt.[a]	71.7	40.7	31.2

[a] [Ref. 39].
[b] [Ref. 56].

$$\Delta E_{tetra} = 6\left(C_{11} - C_{12}\right) V_0 \delta^2 \tag{3}$$

The bulk modulus B_0 is obtained from Murnaghan's equation of state. The first equation contains the relation between the elastic constants (C_{11} and C_{12}) and B_0. The second equation shows the variation of the strain energy (ΔE_{rhomb}) versus the volume-conserving rhombohedral strain (δ). The third equation is related to the variation of the strain energy (ΔE_{tetra}) versus the volume conserving tetragonal strain (δ). The calculated values of the elastic constants for the ZnX compounds are displayed in table 2 and are compared with experimental results [39]. The calculated values agree well with the available experimental data. The elastic constants decrease in magnitude with increase in lattice dimension from ZnS to ZnTe, because of cohesive energy decreases with the nearest-neighbour distance [40]. The structure stability in a cubic crystal requires elastic constants satisfying the conditions $C_{11} - C_{12} > 0$, $C_{44} > 0$, $C_{11} + 2C_{12} > 0$, $C_{12} < B_0 < C_{11}$. From table 2, it can be seen that all these conditions are satisfied. The bulk modulus, B_0, Young's modulus, Y, isotropic shear modulus, G, and Poisson ratio, σ, can be determined from the elastic constants, viz., C_{11}, C_{12} and C_{44}, using the following explicit expressions [41, 42]:

$$G = \left(G_V + G_R\right)/2 \tag{4}$$

where G_V is Voigt's shear modulus and G_R is Reuss's shear modulus for cubic crystals, expressed as:

$$G_V = \frac{C_{11} - C_{12} + 3C_{44}}{5} \tag{5}$$

$$G_R = \frac{5C_{44}\left(C_{11} - C_{12}\right)}{4C_{44} + 3\left(C_{11} - C_{12}\right)} \tag{6}$$

The expressions for the Young's modulus and Poisson's ratio are given by

$$Y = \frac{9GB}{G + 3B} \tag{7}$$

$$\sigma = \frac{3B - 2G}{6B + 2G} \tag{8}$$

Table 3. The calculated values of the elastic modulus for the ZnX compound.

	G (GPa)	B_0/G	C_{12}–C_{44} (GPa)	Y (GPa)	σ
ZnS	41.88662	2.15152	1.88	108.8	0.299
ZnSe	33.41409	2.16735	3.93	86.88	0.3
ZnTe	27.48057	2.19755	7.57	71.584	0.302

Table 3 presents the calculated values of the elastic modulus. The bulk modulus, B_0, is the measure of the resistance to fracture, while the shear modulus, G, is the measure of the resistance to plastic deformation. The ratio B_0/G is an important parameter for the determination of the ductility of the materials [43]. It can be seen from table 3 that the B_0/G ratio for all ZnX compounds is greater than 1.75. This reveals that the compounds are ductile in nature. The highest value of the B_0/G ratio is 2.19 for ZnTe, which indicates that ZnTe is the most ductile among all of the ZnX compounds. The binding properties and the ductility are interlinked [44]. The bond character of cubic compounds is expressed in terms of their Cauchy pressure ($C_{12} - C_{44}$). With an increase in positive Cauchy pressure, a compound is likely to form a metallic bond. The ductile nature of all ZnX compounds can be correlated to their positive Cauchy pressure, with a metallic character in their bonds. ZnTe has the highest positive Cauchy pressure, showing strong metallic bonding (ductility) as compared to other compounds.

The calculated value of Young's modulus (Y) is shown in table 3. Young's modulus provides the degree of stiffness of the solid. A stiffer material has a larger value of Y, and such material possesses covalent bonds. From table 3, it can be seen that the highest value of Y occurs for ZnS. This demonstrates that ZnS is more covalent in nature as compared to other ZnX compounds. Poisson's ratio (σ) is a measure of compressibility. The values of σ for all ZnX compounds are between 0.29 and 0.30, which predicts that all the compounds are compressible. Poisson's ratios with values between 0.25 and 0.5 represent interatomic forces as the central force in solids. In our case, the Poisson's ratios are around 0.3, which reveals that the interatomic forces in the ZnX compounds are central forces.

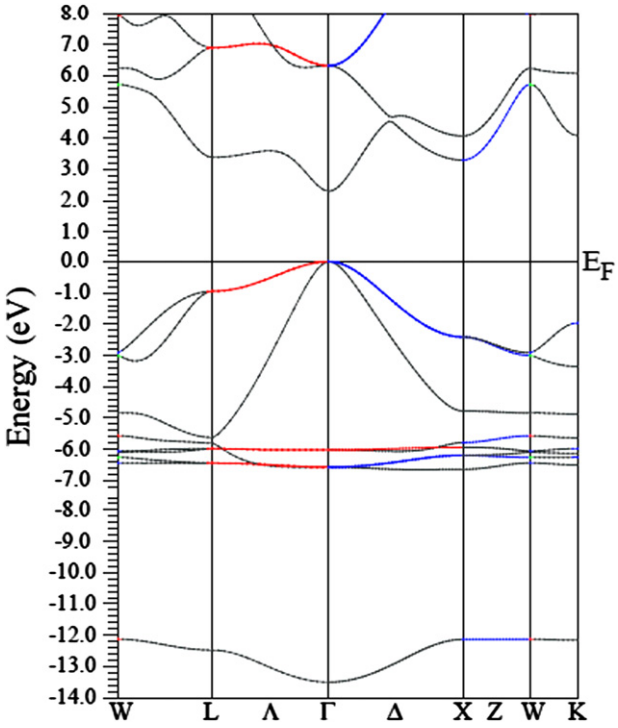

Figure 1. The electronic band structure for ZnS.

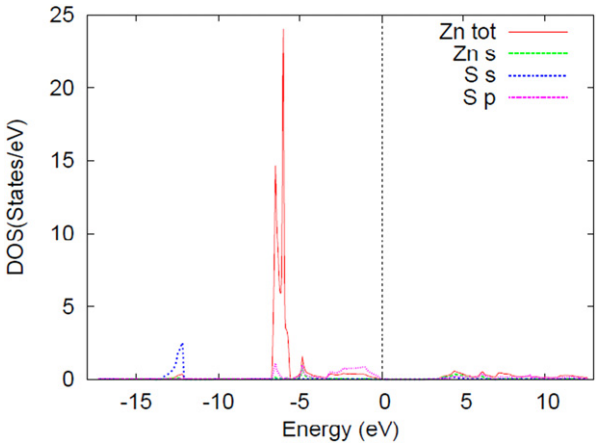

Figure 2. The density of states (DOS) for ZnS.

3.2. Electronic properties

The electronic band structure of Zn chalcogenides has been calculated. The calculated band structure for ZnS at equilibrium is shown in figure 1. ZnS is considered as a prototype since the band structures are quite similar for all three compounds, with little differentiation. The calculated band structure is in good agreement with other theoretical results [45–48].

The zero of the energy scale is set at the top of the valence band (VB). The energy band structures are calculated along the directions containing high symmetry points of the first Brillouin zone, namely $W \rightarrow L \rightarrow \Gamma \rightarrow X \rightarrow W \rightarrow K$. Each member of ZnX demonstrates the existence of the valence band maximum and conduction band minimum at the same symmetry point. This confirms the direct energy gap between the top of the valence band and the bottom of the conduction band at the Γ point. With the increase in the lattice parameters starting from the sulphide to the telluride, the X atom p bands shift up in energy as a common feature of II–VI compounds [49]. The calculated band gap is underestimated in comparison with the experimental results, because of the simple form of GGA which cannot account for the quasiparticle self-energy [50].

The density of states (DOS) for ZnS is shown in figure 2. It is similar to that of ZnSe and ZnTe. The first structure in the total DOS is small and centered at around −12.29 eV, −12.37 eV and −11.18 eV for ZnS, ZnSe and ZnTe, respectively. This structure arises from the chalcogen s states and it

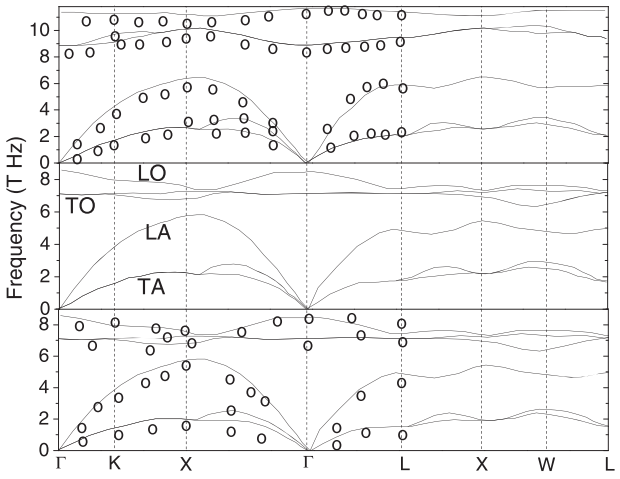

Figure 3. The phonon frequencies of ZnS (top), ZnSe (middle) and ZnTe (bottom) at zero pressure. The circles show the neutron scattering data for ZnS and ZnTe [61].

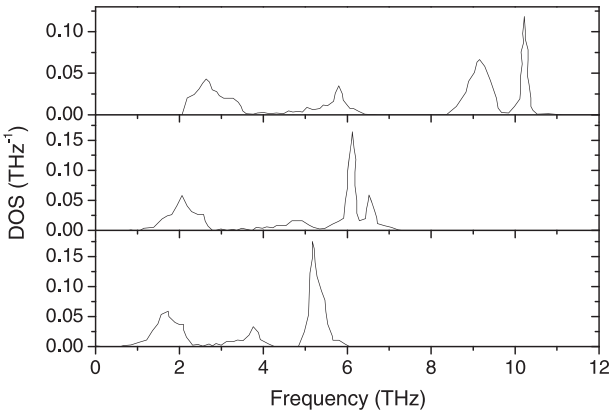

Figure 4. The phonon density of states of ZnS (top), ZnSe (middle) and ZnTe (bottom) at zero pressure.

corresponds to the lowest lying band with the dispersion in the region around the Γ point in the Brillouin zone. The next structure appears at −6.20 eV, −6.56 eV and −7.09 eV for ZnS, ZnSe and ZnTe, respectively. It is an attribute of Zn d states with some p states of the chalcogen atoms, and it occupies the largest number of states with flat bands clustered between −5.6 eV and −6.5 eV (for ZnS). Less dispersion of these bands results in sharp peaks. There is a wide spread in DOS in the energy range of −5.6 eV and zero energy for these compounds. The peaks in this energy interval arise from the chalcogen p states partially mixed with Zn s states, and they contribute to the upper valence band. Above the Fermi level, the feature in the DOS originates mainly from the s and p states of Zn partially mixed with a little of the chalcogen d states. The band width of the valence band as determined from the width of the peaks in a DOS dispersion below the Fermi level is equal to 13.42 eV, 13.13 eV, 12.17 eV for ZnS, ZnSe and ZnTe, respectively. The results showing the valence band width minimum for ZnTe clearly indicate that the wave function for ZnTe is more localized than that for ZnS. This is consistent with the fact that when the atomic number of the anion increases, a material becomes non-polar covalent with valence band states being more localized.

3.3. Dynamical properties

The vibrational frequency, ω, is described with the dispersion relation $\omega = \omega_j$ (q) [51], where j is the branch index. The response of phonon frequencies with the atomic displacements matrix q [12] is used for phonon dispersion spectrum determination [52]. Due to the translational symmetry $\omega_j(q + G) = \omega_j(q)$, we calculate the phonon frequencies in the first Brillouin zone (BZ) only. Figure 3 displays the phonon dispersion relation of ZnX binary semiconductors in the zinc-blende structure along high-symmetry directions. Other calculated and experimental phonon properties are available in the literature for comparison [53–60]. Also, existing inelastic neutron scattering phonon data [61] for ZnS and ZnTe has been compared with calculated phonon dispersion, as shown in figure 3. The dispersion curve shows the symmetry properties in q-space subject to restriction in the first Brillouin zone. The unit cell of the ZnX crystal with 2 atoms contributes to six branches: three acoustical and three optical. The phonon density of states (PDOS) is shown in figure 4. The PDOS of ZnX exhibits one peak between 1 and 3.5 THz, arising essentially from the acoustic phonon branches, and a sharp double peak at higher energies corresponding to the optical phonons. The position of the latter peaks moves towards a lower energy as one substitutes S by Se and Te. These two main peak groups are separated by a gap in which a small mid-gap peak is located. We have calculated the phonon frequencies for the longitudinal optical (LO) and transverse optical (TO) modes along with transverse acoustic (TA) and longitudinal acoustic (LA) modes. A comparative description of our calculated frequencies of optical and acoustic branches with other calculations, at q = 0 (Γ point) and at the point X (1, 0, 0), is given in table 4.

The LO and TO phonons have the frequencies, respectively, of 11.32 THz and 8.82 THz at the zone center (Γ) for ZnS. The LO (Γ) modes for ZnSe and ZnTe, respectively, have the frequencies of 8.59 THz and 7.81 THz. The shapes of the phonon dispersion spectra of ZnX (X = S, Se and Te) compounds are similar to each other. The TO phonon dispersion of ZnX shows flatness. It is flatter for ZnSe and ZnTe and has a relatively sharp peak in the PDOS. Along the direction between the zone centre (Γ) and the zone boundary (X or L), the LO branch shows an upward flat dispersion, which induces a weak peak in the PDOS. The LO and TO branches are clearly separated in all materials. It can be observed in table 4 that our calculated frequency values are somewhat higher than the experimental results, while some other calculations show lower values than the experimental results. For example, in our calculation, the TO (Γ) for ZnS has a frequency of 8.82 THz (6.5% higher than the experimental value) while You Yu *et al* [22] reported the same as 8.01 THz. The difference in the result arises from the fact that our calculation is based on the all-electron method and the latter followed the pseudopotential method [22]. The pseudopotential deals with only valence electrons. As a

Table 4. A comparative description of the calculated frequencies of optical and acoustic branches with other calculations and experimental results, at q = 0 (Γ point) and at the point X (1, 0, 0).

Compound	LO (Γ)	TO (Γ)	LO (X)	TO (X)	LA (X)	TA (X)
ZnS						
Present	11.32	8.82	11.09	10.02	6.19	2.58
Calc.	10.53[a], 10.44[b]	8.1[b], 8.01[c], 8.67[d], 8.28[e]	9.57[c]	9.15[c], 9.33[d]	6.09[c], 6.27[d]	2.52[c], 3.15[d]
Expt.		8.28[f]		9.48[f]	6.33[f]	2.7[f]
ZnSe						
Present	8.59	7.01	7.21	7.13	5.86	2.08
Calc.	7.56[a], 7.35[c]	6.72[d], 5.94[g], 6.18[g], 6.09[g], 6.21[h], 6.15[i], 6.18[a], 6.15[c]	6.36[c]	6.24[c], 6.09[d]	5.52[c], 5.19[d]	2.01[c], 2.37[d]
Expt.		6.39[j]		6.57[j]	5.82[j]	2.1[j]
ZnTe						
Present	7.81	6.86	7.02	6.85	5.19	1.95
Calc.	6.3[k], 6.18[a], 5.64[c]	4.83[c], 6.06[d], 5.43[k], 5.37[a]	5.01[c]	4.59[c], 5.91[d]	3.81[c], 4.56[d]	1.59[c], 2.19[d]
Expt.		5.31[f]		5.55[f]	4.08[f]	2.52[f]

[a] [Ref. 54].
[b] [Ref. 53].
[c] [Ref. 22].
[d] [Ref. 6].
[e] [Ref. 55].
[f] [Ref. 56].
[g] [Ref. 39].
[h] [Ref. 57].
[i] [Ref. 58].
[j] [Ref. 59].
[k] [Ref. 60].

consequence, the valence electrons are described with a relatively small number of basis functions. In this method, the core–valence interaction is kept at the DFT level and pseudo wave functions are used. In our calculation with the all-electron method, the energies are chosen in the respective valence band regime, and the local orbitals are introduced to illustrate semicore states. It offers the flexibility of the basis in case of large band widths. The precise basis sets are able to compute accurate all-electron response functions. This procedure has demonstrated to be very accurate for ground-state calculations.

The mass of the constituent atom in the compound significantly affects the shapes of the dispersion curves of the phonon branches. The contribution to the optical modes from Zn increases on going from S to Te and, for acoustical modes, the contribution from the chalcogen increases on going from S to Te. For the ZnS, the acoustical and the optical phonon branches arise essentially from vibrations of Zn and S, respectively. Because of the mass mismatch between the zinc and chalcogen atoms, the acoustic and optical branches are separated. Due to the large difference in mass between Zn and S, a clear divergence between the acoustical and optical branches is observed. For ZnSe, due to the small difference in the atomic masses of Zn and Se, the acoustical and optical phonon branches result from mixed Zn and Se vibrations with less divergence between the acoustical and optical branches. For the ZnTe, the acoustical phonons arise from Te vibrations and the optical phonons from Zn vibrations. At the zone centre, the LO/TO splittings are 2.62, 1.71 and 1.68 THz for ZnS, ZnSe and ZnTe, respectively. Also at the zone centre, the TO branches for ZnSe and ZnTe are flatter than those for ZnS.

3.4. Thermal properties

According to standard thermodynamics, the Helmholtz free energy at a temperature T in a crystal phase is [62]

$$F\left(\mathbf{Z};\,T\right) = E\left(\mathbf{Z}\right) + F_{el}\left(\mathbf{Z};\,T\right) + F_{vib}\left(\mathbf{Z};\,T\right) \tag{9}$$

where **Z** is the crystal configuration vector, which includes all the relevant geometric information for the crystal structure, i.e., the independent unit cell lengths and angles, and all of the free crystallographic coordinates of the atoms in non-fixed Wyckoff positions. E(**Z**) is the static energy (without zero-point vibrational energy) at 0 K. F_{el}(**Z**, T) and F_{vib}(**Z**, T) are, respectively, the electronic and vibrational contribution to the free energy. As in our case of a semiconducting material, the electronic contribution can be neglected.

Based on a harmonic approximation, F_{vib}(**Z**, T) is described in terms of the phonon density of states as

$$F_{vib}\left(\mathbf{Z};\,T\right) = \int\left[\frac{1}{2}\hbar\omega + k_B T\,\ln\left(1 - e^{-\hbar\omega/k_B T}\right)\right] \times g\left(\mathbf{Z};\,\omega\right)d\omega \tag{10}$$

where g(**Z**; ω) is the phonon density of states. g(**Z**; ω) is estimated in two ways: either by phonon calculations [63, 64]

for the sake of accuracy or by a Debye model [65, 66] for the sake of simplicity. But the crystal geometrical parameters are not considered very explicitly in the Debye model. This very appropriate feature of the model makes it fully independent of any particular crystal structure. In particular, it is sufficient to consider the variation E(V) as a function of volume (V) only, while the crystal energy depends on many internal parameters and arbitrary cell constants. This fact greatly simplifies the thermodynamic study of the crystal, as it is entirely isolated from the microscopical details behind the E(V) variation. As a result, the Debye-model based on the computed bulk modulus [67], and the consequent thermodynamic calculations, differ from the experimental data. In a first-principles thermodynamic study, Shang *et al* [68] showed very good agreement between the phonon calculation and experimental results, whereas at high temperature (~1400 K) there is more than 10% disagreement between the Debye calculation and experimental results. This fact motivates the need of phonon calculations other than Debye's model for thermodynamic study.

The thermodynamic properties of ZnX are obtained from the phonon spectrum. We calculated the Helmholtz free energy, F, entropy, S, and heat capacity, Cv, of the ZnX compounds using the phonon density of states and harmonic approximation as a function of temperature from the following relations:

$$\Delta F = 3nNk_BT\int_0^{\omega_{\max}} \ln\left[2\ \sinh\ \frac{\hbar\omega}{2k_BT}\right] g(\omega)\, d\omega \qquad (11)$$

$$S = 3nNk_B\int_0^{\omega_{max}} \left[\frac{\hbar\omega}{2k_BT}\ \coth\ \frac{\hbar\omega}{2k_BT} - \ln\left\{2\ \sinh\ \frac{\hbar\omega}{2k_BT}\right\}\right] g(\omega)\, d\omega \qquad (12)$$

$$C_V = 3nNk_B\int_0^{\omega_{\max}} \left(\frac{\hbar\omega}{2k_BT}\right)^2 \mathrm{csch}^2\left(\frac{\hbar\omega}{2k_BT}\right) g(\omega)\, d\omega \qquad (13)$$

where n is the number of atoms per unit cell, N is the number of unit cells, k_B is the Boltzmann constant, ω is the phonon frequency, $\omega_{\max}$ is the highest phonon frequency and T is temperature. Here, $g(\omega)$ is the phonon density of states with a normalization of $\int_0^{\omega_{\max}} g(\omega)\, d\omega = 1$. The calculated free energy, entropy and specific heat at different temperatures are shown in figures 5, 6 and 7, respectively.

At a particular temperature, the free energy maintains the relation ZnS > ZnSe > ZnTe, as a consequence of the decrease in average phonon frequencies starting from the sulphide to the telluride. For example, at very low temperature, ΔF, being equal to $\frac{3}{2}nN\hbar\int_0^{\omega_{\max}} \omega g(\omega)\, d\omega$, will have a greater value for ZnS in comparison to ZnSe and ZnTe. At low temperature, the three specific heats show the T^3 power-law dependence. At high temperature, the specific heat data approaches the classical limit of $C_V = 3nk_B = 50$ J/mol K. The trend in the value of the entropy and the specific heat as ZnS < ZnSe < ZnTe over the whole range of temperature can be attributed to

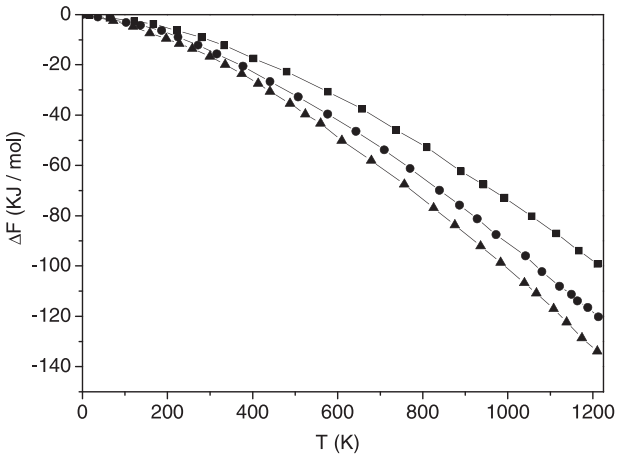

Figure 5. The calculated free energy of ZnX ((■) ZnS, (◆) ZnSe, (▲) ZnTe) at different temperatures.

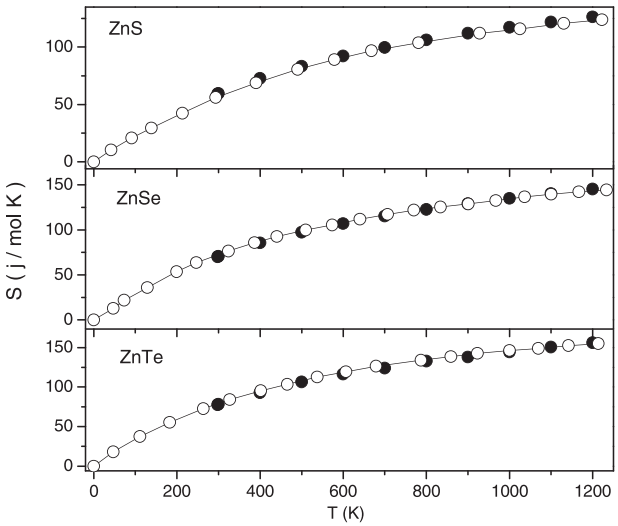

Figure 6. The temperature variation of the entropy of the ZnX compound. (○ are calculated values, ● are from a calorimetric study[59]).

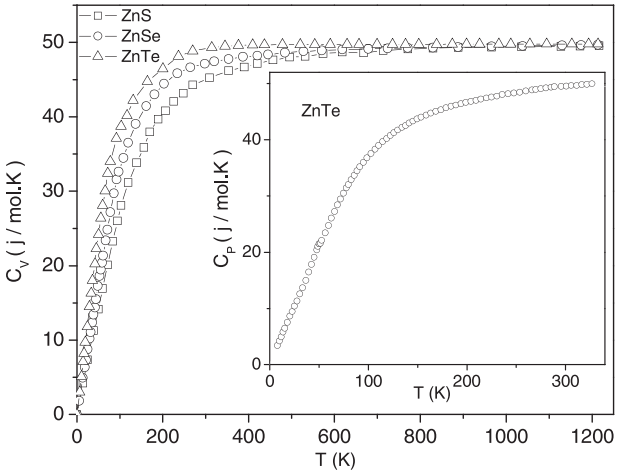

Figure 7. The temperature variation of the constant volume specific heats (C_V) of ZnX (X = S, Se, Te). Inset: The C_P of ZnTe (experimental values [59]).

their phonon density of states for low frequency modes. The lattice contribution to the heat capacity, as shown in figure 7, follows the Debye model at low temperatures and approaches the Dulong–Petit limit at high temperatures (at about room temperature).

4. Conclusions

The electronic, elastic, phonon and thermal properties of Zn-chalcogenides (ZnTe, ZnSe and ZnTe) have been studied with the FP-LAPW+*lo* method in the framework of density functional theory. Quantities such as the elastic constant, phonon dispersion and thermodynamic parameters were obtained. The generalized gradient approximation parameterized by the Perdew, Burke and Ernzerhof (GGA/PBE) method was considered for the exchange and correlation effect calculations. The elastic constants maintained all conditions to be satisfied for the mechanical stability of the compound. The profound ductility in the ZnX compound was observed with the increase in chalcogen atomic number. The metallic character in their bonds was well demonstrated from the positive Cauchy pressure ($C_{12}-C_{44}$) values. The calculated lattice parameters of the ZnX compound are in good agreement with the experimental results, with a 1.56% error. The phonon dispersion curves and corresponding phonon density of states were obtained. The phonon frequencies in the Brillouin zone at different symmetry, Γ, X and L points were estimated. With a harmonic approximation, the phonon contribution to the thermodynamic properties, viz., the Helmholtz free energy ΔF, the entropy S and the constant volume specific heat C_V, were calculated based on the phonon dispersion relations. The calculated thermodynamic properties are in very good agreement with the experimental data.

Acknowledgements

We acknowledge the support in part by the Department of Science and Technology through computing resources provided by the High Performance Computing Facility at the Inter University Accelerator Centre, New Delhi. The first author (B K S) is thankful to Galgotias University, Uttar Pradesh, India, for its support.

References

[1] Tanaka K 1989 *Phys. Rev.* B **39** 1270
[2] Shukla S and Kumar S 2012 *Pramana—J. Phys.* **78** 309
[3] Ohta T 2001 *J. Opto-Electron. Adv. Mater.* **3** 609
[4] Sadekar H K, Deshpande N G, Gudage Y G, Ghosh A, Chavhan S D, Gosavi S R and Sharma R 2008 *J. Alloys Compd.* **453** 519
[5] Yubuta K, Sato T, Nomura A, Haga K and Shishido T 2007 *J. Alloys Compd.* **436** 396
[6] Van L H, Hong M H and Ding J 2008 *J. Alloys Compd.* **449** 207
[7] Wenisch H, Schull K, Homanel D, Landeehr G, Siche D and Hartmann H 1996 *Semicond. Sci. Technol.* **11** 107
[8] Li H and Jie W 2003 *J. Crystal Growth.* **257** 110
[9] Hohenberg H and Kohn W 1964 *Phys. Rev.* **136** B864
[10] Agrawal Bal K, Yadav P S and Agrawal S 1994 *Phys. Rev.* B **50** 14881
[11] Gangadharan R, Jayalakshmi V, Kalaiselvi J, Mohan S, Murugan R and Palanivel B 2003 *J. Alloy. Compd.* **359** 22
[12] Serrano J, Romero A H, Manjón F J, Lauck R, Cardona M and Rubio A 2004 *Phys. Rev.* B **69** 094306
[13] Khenata R, Bouhemadou A, Sahoun M, Reshak Ali H, Baltache H and Rabah M 2006 *Comput. Mater. Sci.* **38** 29
[14] Hassan F El Haj and Akbarzadeh H 2007 *J. Alloys Compd.* **433** 306
[15] Charifi Z, Baaziz H and Reshak Ali H 2007 *Phys. Status Solidi* (b) **244** 3154
[16] Kohn W and Sham L J 1965 *Phys. Rev.* **140** A1133
[17] Laskowski R and Christensen N E 2006 *Phys. Rev.* B **73** 045201
[18] Karazhanov S Z, Ravindran P, Grossner U, Kjekshus A, Fjellvåg H and Svensson B G 2006 *J. Appl. Phys.* **100** 043709
[19] Karazhanov S Z, Ravindran P, Grossner U, Kjekshus A, Fjellvåg H and Svensson B G 2006 *J. Cryst. Growth* **287** 162
[20] Lambrecht W R L, Rodina A V, Limpijumnong S, Segall B and Meyer B K 2002 *Phys. Rev.* B **65** 075207
[21] Lew Yan Voon L C, Willatzen M, Cardona M and Christensen N E 1996 *Phys. Rev.* B **53** 10703
[22] Yu Y, Zhou J, Han H, Zhang C, Cai T, Song C and Gao T 2009 *J. Alloys. Comp.* **471** 492
[23] Betzinger M, Friedrich C, Görling A and Blüge S 2012 *Phys. Rev.* B **85** 245124
[24] Gonze X and Lee C 1997 *Phys. Rev.* B **55** 10355
[25] Kresse G, Furthmüller J and Hafner J 1995 *Europhys. Lett.* **32** 729
[26] Blaha P, Schwarz K, Sorantin P and Rickey S B 1990 *Comput. Phys. Commun.* **59** 399
[27] Perdew J P, Burke K and Ernzerhof M 1996 *Phys. Rev. Lett.* **77** 3865
[28] Murnaghan F D 1944 *Proc. Natl. Acad. Sci. USA* **30** 382
[29] Monkhorst H J and Pack J D 1976 *Phys. Rev.* B **13** 5188
[30] Togo Atsushi, Fumiyasu Oba and Tanaka Isao 2008 *Phys. Rev.* B **78** 134106
[31] Gürel H H, Akinci Ö and Ünlü H 2012 *Superlattices Microstruct.* **51** 725
[32] Boutaiba F, Zaoui A and Ferhat M 2009 *Superlattices Microstruct.* **46** 823
[33] Wei S H and Zunger A 1988 *Phys. Rev.* B **37** 8958
[34] Schowalter M, Lamoen D and Rosenauer A 2004 *Appl. Phys. Lett.* **85** 4938
[35] Chen X, Mintz A, Hu J, Hua X and Zinck J 1995 *J. Vac. Sci. Technol.* B **13** 4
[36] Wei S H and Zunger A 1999 *Phys. Rev.* B **60** 5405
[37] Postnikov AV, Pagès O and Hugel J 2005 *Phys. Rev.* B **71** 115206
[38] Blaha P, Schwarz K, Madsen G K H, Kvasnicka D and Luitz D 2001 *WIEN2k, An Augmented Plane Wave Plus Local Orbitals Program for Calculating Crystal Properties* (Austria: Vienna University of Technology)
[39] Lee B H 1970 *J. Appl. Phys.* **41** 2988
[40] Verma A S, Sarkar B K and Jindal V K 2010 *Pramana* **74** 851
[41] Voigt W 1889 *Ann. Phys.* **38** 573
[42] Reuss A and Angew Z 1929 *Math. Phys.* **9** 49
[43] Pugh S F 1954 *Phil. Mag.* **45** 823
[44] Ganeshan S, Shang S L, Zhang H, Wang Y, Mantina M and Liu Z K 2009 *Intermetallics* **17** 313
[45] Adachi S and Taguchi T 1991 *Phys. Rev.* B **43** 9569

[46] Christensen N E and Christensen O B 1986 *Phys. Rev.* B **33** 4739
[47] Ghahramani E D, Moss D J and Sipe J E 1991 *Phys. Rev.* B **43** 9700
[48] Lee G D, Lee M H and Ihm J 1995 *Phys. Rev.* B **52** 1459
[49] Wei S H and Zunger A 1996 *Phys. Rev.* B **53** R10457
[50] Rashkeev S N and Lambrecht W R L 2001 *Phys. Rev.* B **63** 165212
[51] Omar M A 1975 *Elementary Solid State Physics: Principles and Applications* (Reading, Massachusetts: Addison-Wesley Publishing Company)
[52] Duan Y H and Parlinski K 2011 *Phys. Rev.* B **84** 104113
[53] Karazhanov S ZH, Ravindran P, Kjekshus A, Fjellvag H and Svensson B G 2007 *Phys. Rev.* B **75** 155104
[54] Ves S, Schwarz U, Christensen N E, Syassen K and Cardona M 1990 *Phys. Rev.* B **42** 9113
[55] Madelung O (ed) 1982 *Numerical Data and Functional Relationship in Science and Technology, Landolt_Börnstein* (*New Series Group III* vol 17) (Berlin: Springer-Verlag)
[56] Jansiukiewicz C and Karpus V 2003 *Solid State Commun.* **128** 167
[57] Casali R A and Christensen N E 1998 *Solid State Commun.* **108** 793
[58] Okoye C M I 2003 *Physica* B **337** 1
[59] Barin I 1995 *Thermochemical Data of Pure Substances* 3rd edn (New York: VCH)
[60] Peterson D L, Petrou A, Giriat W, Ramdas A K and Rodriguez S 1986 *Phys. Rev.* B **33** 1160
[61] Weinstein B A 1977 *Solid State Commun.* **24** 595
[62] Maradudin A A, Montroll E W, Weiss G H and Ipatova I P 1971 *Theory of Lattice Dynamics in the Harmonic Approximation* (Academic Press) Q3
[63] Hu W C, Liu Y, Li D J, Zeng X Q and Xu C S 2013 *Physica* B **427** 85
[64] Gupta S D, Jha P K and Pandya A 2013 *Solid State Sciences* **21** 66
[65] Lu Y and Zhang P 2014 **82** 5 Q4
[66] Feng S, Li S and Fu H 2014 *Comp. Mater. Sci.* **82** 45
[67] Liu Y, Hu W C, Li D J, ZengX Q, Xu C S and Yang X J 2014 *Physica* B **432** 33
[68] Shang S L, Wang Y, Kim D E and Liu Z K 2010 *Comput. Mater. Sci.* **47** 1040

QUERY FORM

JOURNAL: Physica Scripta

AUTHOR: B K Sarkar *et al*

TITLE: First-principles calculations of the structural, phonon and thermal properties of ZnX (X = S, Se, Te) chalcogenides

Q1

ARTICLE ID: ps479978

Columns may not have been fully balanced and matched in this proof, this will be done once final corrections have been incorporated.

SQ1
Author: Please be aware that the colour figures in this article will only appear in colour in the online version. If you require colour in the printed journal and have not previously arranged it, please contact the Production Editor now.

Page 10

Q1
please read your edited paper carefully to check that our changes have not altered your intended meaning. Amendments have been made throughout for reasons of clarity, readability, grammar and consistency of tenses.

Page 4

Q2
please check that I haven't changed your meaning in the edited sentence: "The ductile nature of all ZnX compounds can be correlated to their positive Cauchy pressure, with a metallic character in their bonds."

Page 8

Q5
Please check the details for any journal references that do not have a link as they may contain some incorrect information.

Page 9

Q3
Publisher location and name are required for book references. Please provide the missing information.

Page 9

Q4
Please check if this reference is to a book, journal conference proceedings or other and supply the complete details as appropriate.